

Blue-detuned molecular magneto-optical trap schemes based on bayesian optimization

S. Xu,¹ R. Li,¹ Y. Zhai,^{2,3,4,*} Y. Xia,^{5,†} M. Siercke,⁶ and S. Ospelkaus⁶

¹National Institute of Extremely-Weak Magnetic Field Infrastructure, Hangzhou, 310052, China

²Key Laboratory of Ultra-Weak Magnetic Field Measurement Technology, Ministry of Education, School of Instrumentation and Optoelectronic Engineering, Beihang University, Beijing, 100191, China

³Zhejiang Provincial Key Laboratory of Ultra-Weak Magnetic-Field Space and Applied Technology, Hangzhou Innovation Institute, Beihang University, Hangzhou, 310051

⁴Hefei National Laboratory, Hefei, 230088, China

⁵State Key Laboratory of Precision Spectroscopy, School of Physics and Electronic Science, East China Normal University, Shanghai 200241, China

⁶Institut für Quantenoptik, Leibniz Universität Hannover, 30167 Hannover, Germany

Direct laser cooling and trapping of molecules to temperature below Doppler limit and density exceeding 10^8 are challenging due to the sub-Doppler heating effects of molecular magneto-optical trap (MOT). In our previous paper [1], we presented a general approach to engineering the sub-Doppler force by tuning the AC stark shift with the addition of a blue detuned laser. Here, by employing the Bayesian optimization method to optical Bloch equations, we have identified multiple blue-detuned MOT schemes for the CaF molecule. From the three-dimensional Monte-Carlo simulation, we obtained a MOT temperature and density of $14\ \mu\text{K}$ and $4.5 \times 10^8\ \text{cm}^{-3}$, respectively. Our findings present a potential avenue for directly loading molecular MOTs into conservative traps, which can capitalize on the high density and low temperature of the MOT

Recent experiments using molecular magneto-optical traps (MOT) have been found to suffer from the sub-Doppler heating effects caused by the complex energy levels involved [2, 3]. These effects lead to higher temperature and lower density in the resulting molecular cloud [4–7]. While blue-detuned molasses can effectively cool molecules to temperatures as low as a few μK [8–13], they are not suited to compressing or increasing the density of the MOT. The successful implementation of a blue-detuned MOT using type II transition in Rb atoms is a good indication that this technique should work in molecules as well [14]. However, the close hyperfine splittings of molecule result in the interaction of one laser component with all energy levels, which makes it impossible to directly replicate the technique used in atomic MOT. Recently, the YO molecule’s distinctive energy level structure has enabled the successful implementation of a blue-detuned MOT [15], in which the phase-space density is increased by two orders of magnitude. In this paper, we describe the utilization of Bayesian optimization to aid in the discovery of blue-detuned MOT schemes for CaF molecules. We have successfully developed two separate MOT schemes for the $\sigma^-\sigma^-\sigma^+\sigma^-$ and $\sigma^+\sigma^+\sigma^+\sigma^-$ DC MOT configurations that are capable of providing cooling within 5 m/s and trapping within a 3 mm radius. We also discovered a scheme that utilizes only two laser components to achieve a competitive MOT force, which will simplify the experiment significantly. Monte-Carlo simulation with the MOT force results in a significant reduction in temperature and a corresponding increase in density, which can facilitate the transfer of a large number of molecules to conservative

trap [12, 13, 16–19] and thus enhance the effects of subsequent cooling such as evaporative or sympathetic cooling [20–24].

Fig. 1 shows the energy level structure of CaF molecule along with the parameters that require optimization. The $X^2\Sigma^+$ ground state consists of four hyperfine states, namely $F = 1, 0, 1$ and 2 , with corresponding energy splittings of 76 MHz, 47 MHz and 25 MHz, separately. On the other hand, the $A^2\Pi_{1/2}$ excited state has only two hyperfine states, namely $F' = 0$ and 1 , and the energy difference between them is set to 5 MHz [25]. The dashed lines correspond to the four laser components that aim to target the four ground hyperfine states and the upward-pointing arrows indicate the transition to the excited $F' = 1$ state. Starting from the bottom, the four laser components are identified as L_1, L_2, L_3 and L_4 . Each of these components is associated with a specific polarization, detuning, and laser intensity ratio. To narrow down the parameter search space, we limit the polarization to $\sigma^-\sigma^-\sigma^+\sigma^-$ and $\sigma^+\sigma^+\sigma^+\sigma^-$ ($\sigma^-\sigma^-\sigma^+\sigma^-$ and $\sigma^+\sigma^+\sigma^+\sigma^-$ denote that L_1, L_2, L_3 and L_4 have a polarization of $\sigma^-\sigma^-\sigma^+\sigma^-$ and $\sigma^+\sigma^+\sigma^+\sigma^-$, respectively), since both of them are implemented in experiment [4, 5]. The laser beam has a total power of 100 mW and a radius of 7.5 mm in all directions. The magnetic field gradient remains fixed at 15 G/cm. For $\sigma^-\sigma^-\sigma^+\sigma^-$ configuration, we refer to the [4] MOT scheme, in which a single laser modulated by an electric-optic modulator (EOM) generates the L_1, L_2 and L_4 laser components with a modulation frequency of 74.5 MHz. L_3 has a distinct polarization that is generated by an acousto-optic modulator (AOM). In total, we have five free parameters, as shown in the picture, with their tuning ranges. We attempted two different schemes for the $\sigma^+\sigma^+\sigma^+\sigma^-$ configuration. The first scheme involved restricting the laser intensity ratio to be equal, resulting in four different detunings as the

* yueyangzhai@buaa.edu.cn

† yxia@phy.ecnu.edu.cn

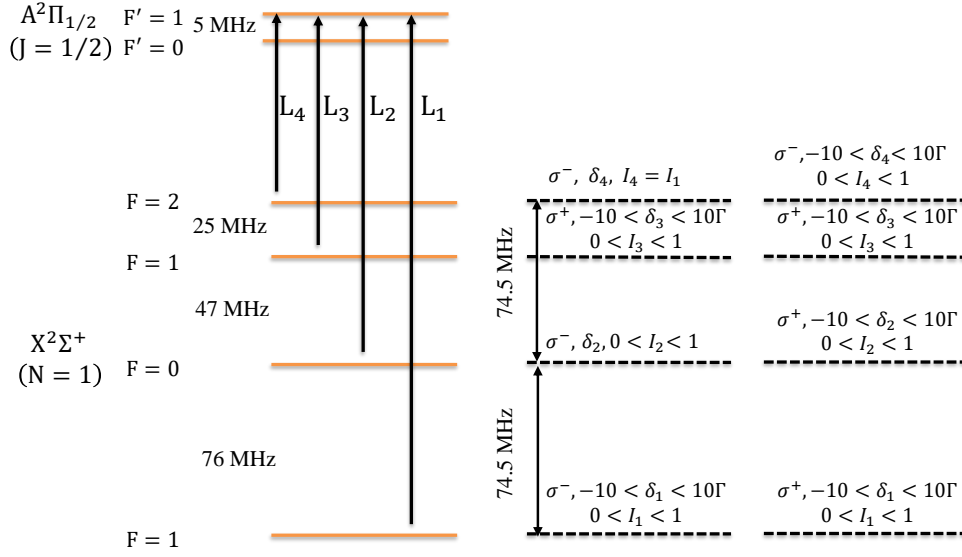


FIG. 1. The energy levels of CaF and the MOT configurations require optimization. The detuning of each laser component can vary between -10 to 10Γ , while the intensity ratio can range from 0 to 1. In the $\sigma^- \sigma^- \sigma^+ \sigma^-$ configuration, there are five free parameters, with δ_2 and δ_4 adjusting based on the modulation frequency of 74.5 MHz and the energy splittings of the hyperfine states. On the other hand, the $\sigma^+ \sigma^+ \sigma^+ \sigma^-$ configuration has eight free parameters, which can be reduced to four if the laser intensity ratio is set equally

only free parameters. The second scheme included eight free parameters, which comprised the detunings and the laser intensity ratio.

Prior to beginning the optimization process, it is necessary to establish a clear goal for the program. This is because we must strike a balance between two types of MOT forces: the cooling force, which depends on ve-

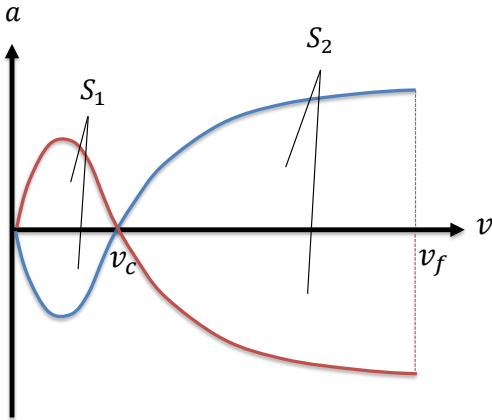


FIG. 2. A red (blue) detuned MOT typically follows a cooling acceleration curve that involves sub-Doppler heating (cooling) in the low velocity range and Doppler cooling (heating) in the high velocity range. The critical velocity, denoted as v_c , marks the point at which the force sign changes. We typically calculate the velocity range $v_f = \Gamma/k$, where Γ is the natural linewidth of the molecular transition and k is the wave vector of the lasers

locity, and the trapping force, which is dependent on space. We initially anticipate a cooling acceleration curve similar to that shown in Fig. 2. This curve exhibits two distinct indications of force for red (blue) detuning: sub-Doppler heating (cooling) in the low velocity range, and Doppler cooling (heating) in the high velocity range. In order to quantify the effectiveness of cooling acceleration with a single value, we employ two integrals: $S_1 = \sum_{v=0}^{v_c} a \Delta v$ and $S_2 = \sum_{v=v_c}^{v_f} a \Delta v$. These integrals are used to calculate a metric for the quality of cooling acceleration, represented as $f_v = (10S_1 + S_2)/v_f$. We assign a weight of 10 to S_1 to highlight its significance, otherwise the program prefers to increasing the S_2 part instead of decreasing the S_1 part. The effectiveness of trapping acceleration f_z is determined solely by the average value obtained within the range of 0 to 3 mm. We attempt to define the final goal for the program in two different ways. In the first approach, we optimize the program separately to attain the maximum cooling and trapping acceleration f_{vm} and f_{zm} . Then, we establish a final result of $R = (f_v/f_{vm}) + (f_z/f_{zm})$ for the program to execute. Alternatively, in the second approach, we assign a dimensionless value of $R = f_v * f_z$ for the program to execute. After conducting multiple tests, we have determined that the second method yields better results and enables us to efficiently and consistently identify the optimal group of parameters.

In order to capture the sub-Doppler force of the MOT, we run the optical Bloch equations (OBEs) [3] for a sufficient amount of time until it reaches a quasi-steady state. We also select Julia as our simulation program to enhance the running speed. Bayesian optimization

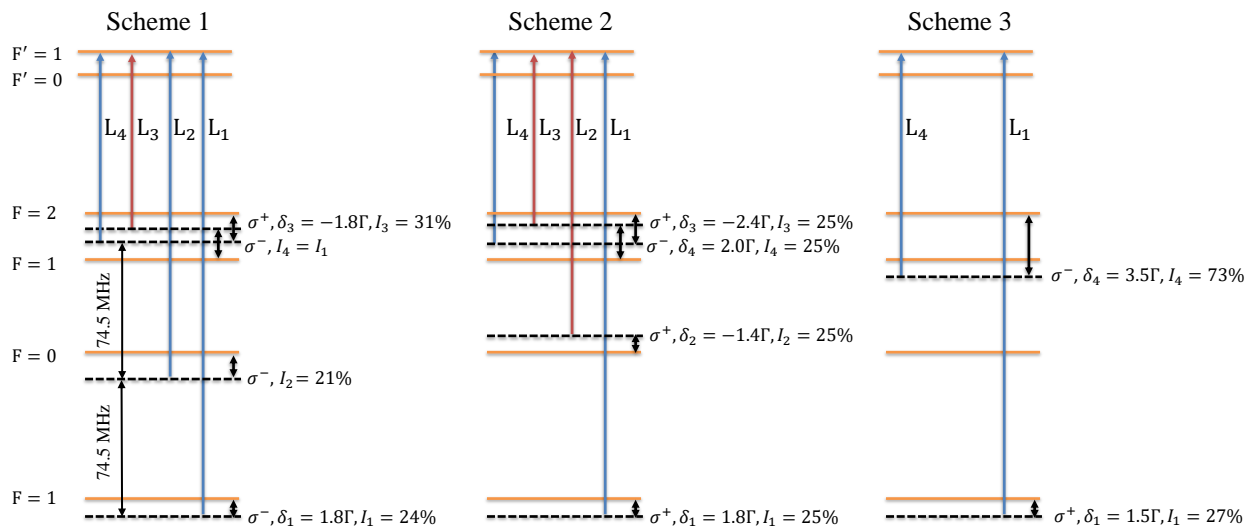


FIG. 3. The blue-detuned MOT schemes for the CaF molecule discovered using Bayesian optimization. Scheme 1 corresponds to the $\sigma^- \sigma^- \sigma^+ \sigma^-$ configuration, while Scheme 2 corresponds to the $\sigma^+ \sigma^+ \sigma^+ \sigma^-$ configuration. Scheme 3 represents the configuration with two laser components. The blue (red) upward arrows indicate the blue (red) detuning relative to the target energy levels. The detunings and laser intensity ratios are labeled in the figure.

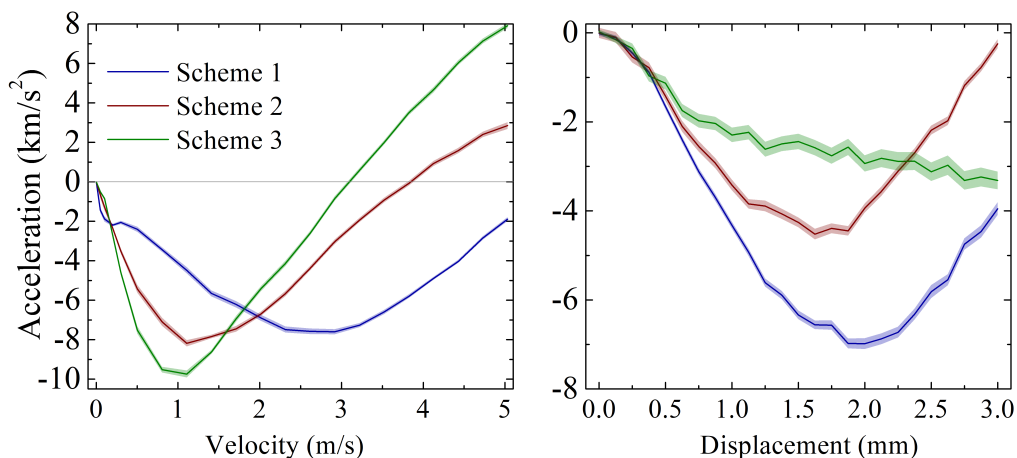


FIG. 4. The acceleration curves for the optimal MOT schemes, showing the velocity-dependent force calculated up to Γ/k (~ 5 m/s) and the trapping force calculated up to 3 mm along the z direction. All schemes can effectively compress and cool the molecules within the MOT center. The shaded areas represent the 68% confidence interval based on 100 and 1000 runs of OBEs for the cooling and trapping forces, respectively

can be implemented using the Scikit-Optimize Python package, and can be called in a Julia environment using the PyCall package. Fig. 3 illustrates the blue-detuned MOT schemes we have found for CaF molecule. As we didn't observe any significant improvement when using eight free parameters in the $\sigma^+ \sigma^+ \sigma^+ \sigma^-$ configuration, for experimental convenience, we only display the results obtained with equal laser intensity. It is evident that in the $\sigma^- \sigma^- \sigma^+ \sigma^-$ configuration, L_1 is detuned by 1.8Γ with respect to the lower $F = 1$ to $F' = 1$ transition and has an intensity ratio of 24%. The detuning of L_2 and L_4 is dependent on the modulation frequency of 74.5 MHz

and the energy splittings. L_2 has an intensity ratio of 21%, whereas the intensity of L_4 is equal to that of L_1 . L_3 is red detuned by -1.8Γ relative to the upper $F = 1$ to $F' = 1$ transition and has an intensity of 31%. The corresponding acceleration curve is illustrated in Fig. 4, where we calculate the velocity-dependent force up to Γ/k at the center of the MOT, and the space-dependent force along the z direction up to a distance of 3 mm, considering a velocity of 0.1 m/s. We observe that the cooling acceleration in Scheme 1 remains negative and strong up to 5 m/s, with a slight bump at 0.2 m/s. Concurrently, the trapping acceleration exhibits a persistent

strength within the computed range. During our search process, we notice that the program consistently generates a strong MOT force even when the parameters fluctuate around the optimal values. This indicates the robustness of our results. Hence, for experimental convenience, it is possible to set the laser intensity equally on all four ground states, which should still yield satisfactory result. In the $\sigma^+\sigma^+\sigma^+\sigma^-$ configuration, we observe a similar arrangement of detunings near the upper $F=2$ and $F=1$ states with minor deviations. Additionally, δ_2 is switched from a blue detuning to a red one. The cooling force of Scheme 2 is more potent until 2 m/s and has a critical velocity of 3.8 m/s. However, we find that Scheme 2 has a peak trapping acceleration that is 64% of that in Scheme 1. During our search process, we noticed that even using a small laser intensity for the L_2 and L_3 laser components, a strong cooling and trapping force can still be achieved. This observation motivated us to explore a search with only two laser components, namely L_1 and L_4 , along with free detunings and laser intensity ratio. Scheme 3 represents the optimal result we discovered. It's different from the Λ -enhanced cooling [10] where equal detunings and laser intensity are used for L_1 and L_4 laser. Additionally, we verified that Λ -enhanced cooling scheme is unable to provide a trapping force. Scheme 3 exhibits the strongest cooling force within the range of 2 m/s and has a critical velocity of 3.1 m/s. Additionally, we observe that the trapping acceleration slope near the MOT center tends to be zero for all the optimal schemes we have identified.

Finally, we make a 3D Monte-Carlo simulation [1] with the calculated MOT force for a total of 10^4 molecules with a uniform velocity distribution within 1 m/s and a uniform distribution of molecules within a radius of 3

mm. Scheme 1 yields a MOT temperature of 90 μK and a density of $4.5 \times 10^8 \text{ cm}^{-3}$, while Scheme 2 produces a temperature of 66 μK and a density of $4.6 \times 10^8 \text{ cm}^{-3}$. Scheme 3 achieves the lowest temperature of 14 μK with a density of $4.5 \times 10^8 \text{ cm}^{-3}$. By reducing the laser power and increasing the field gradient, it should be possible to further improve the system and achieve a temperature as low as several μK [14] while increasing the density even further. This would provide an ideal starting point for transferring a large number of molecules to a conservative trap.

In conclusion, we have presented a general approach for designing a CaF molecular MOT using Bayesian optimization. Our study has yielded three blue-detuned MOT configurations capable of achieving sub-Doppler cooling within 5 m/s and trapping within 3 mm. Monte-Carlo simulations demonstrate that our MOT schemes can achieve a temperature as low as 14 μK and a density as high as $4.5 \times 10^8 \text{ cm}^{-3}$. Our methodology is not limited to CaF molecules but can be adapted to other laser-cooled molecules with varying energy level structures to improve their molecular MOT design.

ACKNOWLEDGEMENTS

This work was supported by the Innovation Program for Quantum Science and Technology (Grant Nos. 2021ZD0300500 and 2021ZD0300503). Y. Xia gratefully acknowledge the financial support from the National Natural Science Foundation of China under Grant Nos. 11834003 and 91836103. M. Siercke and S. Ospelkaus gratefully acknowledge financial support through Germany's Excellence Strategy – EXC-2123/1 Quantum-Frontiers.

-
- [1] S. Xu, P. Kaebert, M. Stepanova, T. Poll, M. Siercke, and S. Ospelkaus, "Engineering the sub-doppler force in magneto-optical traps," *Phys. Rev. Res.* **4**, L042036 (2022).
 - [2] J A Devlin and M R Tarbutt, "Three-dimensional doppler, polarization-gradient, and magneto-optical forces for atoms and molecules with dark states," *New Journal of Physics* **18**, 123017 (2016).
 - [3] J. A. Devlin and M. R. Tarbutt, "Laser cooling and magneto-optical trapping of molecules analyzed using optical bloch equations and the fokker-planck-kramers equation," *Phys. Rev. A* **98**, 063415 (2018).
 - [4] H J Williams, S Truppe, M Hambach, L Caldwell, N J Fitch, E A Hinds, B E Sauer, and M R Tarbutt, "Characteristics of a magneto-optical trap of molecules," *New Journal of Physics* **19**, 113035 (2017).
 - [5] Loïc Anderegg, Benjamin L. Augenbraun, Eunmi Chae, Boerge Hemmerling, Nicholas R. Hutzler, Aakash Ravi, Alejandra Collopy, Jun Ye, Wolfgang Ketterle, and John M. Doyle, "Radio frequency magneto-optical trapping of caf with high density," *Phys. Rev. Lett.* **119**, 103201 (2017).
 - [6] J. F. Barry, D. J. McCarron, E. B. Norrgard, M. H. Steinecker, and D. DeMille, "Magneto-optical trapping of a diatomic molecule," *Nature* **512**, 286–289 (2014).
 - [7] Alejandra L. Collopy, Shiqian Ding, Yewei Wu, Ian A. Finneran, Loïc Anderegg, Benjamin L. Augenbraun, John M. Doyle, and Jun Ye, "3d magneto-optical trap of yttrium monoxide," *Phys. Rev. Lett.* **121**, 213201 (2018).
 - [8] S. Truppe, H. J. Williams, M. Hambach, L. Caldwell, N. J. Fitch, E. A. Hinds, B. E. Sauer, and M. R. Tarbutt, "Molecules cooled below the doppler limit," *Nature Physics* **13**, 1173–1176 (2017).
 - [9] L. Caldwell, J. A. Devlin, H. J. Williams, N. J. Fitch, E. A. Hinds, B. E. Sauer, and M. R. Tarbutt, "Deep laser cooling and efficient magnetic compression of molecules," *Phys. Rev. Lett.* **123**, 033202 (2019).
 - [10] Lawrence W. Cheuk, Loïc Anderegg, Benjamin L. Augenbraun, Yicheng Bao, Sean Burchesky, Wolfgang Ketterle, and John M. Doyle, " Λ -enhanced imaging of molecules in an optical trap," *Phys. Rev. Lett.* **121**, 083201 (2018).
 - [11] Shiqian Ding, Yewei Wu, Ian A. Finneran, Justin J. Bura, and Jun Ye, "Sub-doppler cooling and compressed trapping of yo molecules at μK temperatures," *Phys.*

- Rev. X **10**, 021049 (2020).
- [12] Thomas K. Langin, Varun Jorapur, Yuqi Zhu, Qian Wang, and David DeMille, “Polarization enhanced deep optical dipole trapping of Λ -cooled polar molecules,” Phys. Rev. Lett. **127**, 163201 (2021).
- [13] Yukai Lu, Connor M. Holland, and Lawrence W. Cheuk, “Molecular laser cooling in a dynamically tunable repulsive optical trap,” Phys. Rev. Lett. **128**, 213201 (2022).
- [14] K. N. Jarvis, J. A. Devlin, T. E. Wall, B. E. Sauer, and M. R. Tarbutt, “Blue-detuned magneto-optical trap,” Phys. Rev. Lett. **120**, 083201 (2018).
- [15] Justin J. Burau, Parul Aggarwal, Kameron Mehling, and Jun Ye, “Blue-detuned magneto-optical trap of molecules,” Phys. Rev. Lett. **130**, 193401 (2023).
- [16] H. J. Williams, L. Caldwell, N. J. Fitch, S. Truppe, J. Rodewald, E. A. Hinds, B. E. Sauer, and M. R. Tarbutt, “Magnetic trapping and coherent control of laser-cooled molecules,” Phys. Rev. Lett. **120**, 163201 (2018).
- [17] Loïc Anderegg, Benjamin L. Augenbraun, Yicheng Bao, Sean Burchesky, Lawrence W. Cheuk, Wolfgang Ketterle, and John M. Doyle, “Laser cooling of optically trapped molecules,” Nature Physics **14**, 890–893 (2018).
- [18] Yewei Wu, Justin J. Burau, Kameron Mehling, Jun Ye, and Shiqian Ding, “High phase-space density of laser-cooled molecules in an optical lattice,” Phys. Rev. Lett. **127**, 263201 (2021).
- [19] D. J. McCarron, M. H. Steinecker, Y. Zhu, and D. DeMille, “Magnetic trapping of an ultracold gas of polar molecules,” Phys. Rev. Lett. **121**, 013202 (2018).
- [20] Harald F. Hess, “Evaporative cooling of magnetically trapped and compressed spin-polarized hydrogen,” Phys. Rev. B **34**, 3476–3479 (1986).
- [21] M. H. Anderson, J. R. Ensher, M. R. Matthews, C. E. Wieman, and E. A. Cornell, “Observation of bose-einstein condensation in a dilute atomic vapor,” Science **269**, 198–201 (1995).
- [22] K. B. Davis, M. O. Mewes, M. R. Andrews, N. J. van Druten, D. S. Durfee, D. M. Kurn, and W. Ketterle, “Bose-einstein condensation in a gas of sodium atoms,” Phys. Rev. Lett. **75**, 3969–3973 (1995).
- [23] Hyungmok Son, Juliana J. Park, Wolfgang Ketterle, and Alan O. Jamison, “Collisional cooling of ultracold molecules,” Nature **580**, 197–200 (2020).
- [24] Alisdair O. G. Wallis and Jeremy M. Hutson, “Production of ultracold nh molecules by sympathetic cooling with mg,” Phys. Rev. Lett. **103**, 183201 (2009).
- [25] M. R. Tarbutt and T. C. Steimle, “Modeling magneto-optical trapping of caf molecules,” Phys. Rev. A **92**, 053401 (2015).